Ecological Engineering 114 (2018) 104–114

Contents lists available at ScienceDirect

Ecological Engineering

journal homepage: www.elsevier.com/locate/ecoleng

Temporal dynamics of CO_2 and CH_4 loss potentials in response to rapid hydrological shifts in tidal freshwater wetland soils

Taniya RoyChowdhury[a,*], Lisa Bramer[b], David W. Hoyt[a], Young-Mo Kim[a], Thomas O. Metz[a], Lee Ann McCue[a], Heida L. Diefenderfer[c], Janet K. Jansson[a], Vanessa Bailey[a,*]

[a] Earth and Biological Sciences Directorate, Pacific Northwest National Laboratory, United States
[b] National Security Directorate, Pacific Northwest National Laboratory, United States
[c] Energy and Environment Directorate, Pacific Northwest National Laboratory, United States

ARTICLE INFO

Article history:
Received 22 December 2016
Received in revised form 17 June 2017
Accepted 20 June 2017
Available online 27 June 2017

Keywords:
Anaerobic respiration
Tidal wetlands
Methane production
Sulfate reduction
Iron reduction
Soil metabolites

ABSTRACT

Earth System Models predict climate extremes that will impact regional and global hydrology. Aquatic-terrestrial transition zones like wetlands are subjected to the immediate consequence of climate change with shifts in the magnitude and dynamics of hydrologic flow. Such fluctuating hydrology can alter the nature and rate of biogeochemical transformations and significantly impact the carbon balance of the ecosystem. We tested the impacts of fluctuating hydrology and, specifically, the role of antecedent moisture conditions in determining the dominant carbon loss mechanisms in soils sampled from a tidal freshwater wetland system in the lower Columbia River, WA, USA. Our objective was to understand shifts in biogeochemical processes in response to changing soil moisture, based on soil respiration and methane production rates, and to elucidate such responses based on the observed electron acceptor and metabolite profiles under laboratory conditions. Metabolomics and biogeochemical process rates provided evidence that soil redox was the principal factor driving metabolic function. Fluctuating redox conditions altered terminal electron acceptor and donor availability and recovery strengths of their concentrations in soil such that a disproportionate release of carbon dioxide stemmed from alternative anaerobic degradation processes like sulfate and iron reduction compared to carbon loss due to methanogenesis. Our results show that extended and short-term saturation created conditions conducive to increasing metabolite availability for anaerobic decomposition processes, with a significant lag in methanogenesis. In contrast, extended drying caused a cellular-level stress response and rapid recycling of alternate electron acceptors.
© 2017 Battelle Memorial Institute. Published by Elsevier B.V. This is an open access article under the CC BY-NC-ND license (http://creativecommons.org/licenses/by-nc-nd/4.0/).

1. Introduction

Tidally-driven freshwater coastal vegetated wetland systems are currently estimated to store 870 million metric ton or approximately 1 Pg C within the top 1 m of soil, are highly vulnerable to carbon (C) loss through greenhouse gasses like carbon dioxide (CO_2) and methane (CH_4), as result of reduced precipitation and/or sea-level rise (Kirwan et al., 2013; Kirwan and Megonigal, 2013). Notably, the quantitative uncertainties in estimates of CH_4 emissions from vegetated coastal wetlands are ~30%, respectively (EPA, 2017). The directionality and magnitude of changes in C source-sink strengths of these soils remain uncertain as global climate continues to change.

Earth system models predict frequent extreme weather events with longer dry spells or more variable precipitation intensities at regional and global scales (Jentsch et al., 2007; IPCC, 2013), which will significantly influence terrestrial biogeochemical transformations. Soil microbial communities carry out key ecosystem functions, including biogeochemical cycling of major elements like sulfur and iron coupled to the C cycle. These coupled-C processes can be significantly impacted by changes in the abiotic environment, e.g. reduced oxygen availability in saturated soils or complete aeration of soil due to drought. Although well-known functional guilds of bacteria and archaea drive these processes, we lack understanding of their interrelationships to hydrology-driven shifts in the availability of substrate/metabolites and electron acceptors. Predictions of soil C efflux based on current-climate observations will be invalid under altered precipitation regimes without a mechanistic knowledge of key microbially-mediated C-loss processes, at the level of metabolic pathways, to be able to constrain uncertainties (Wieder et al., 2013; Martiny et al., 2017).

* Corresponding authors.
E-mail addresses: taniya.roychowdhury@pnnl.gov, rctaniya@gmail.com (T. RoyChowdhury), vanessa.bailey@pnnl.gov (V. Bailey).

https://doi.org/10.1016/j.ecoleng.2017.06.041
0925-8574/© 2017 Battelle Memorial Institute. Published by Elsevier B.V. This is an open access article under the CC BY-NC-ND license (http://creativecommons.org/licenses/by-nc-nd/4.0/).

The emissions of carbon dioxide (CO_2) and/or methane (CH_4) are driven by local soil conditions, however the responses vary widely. For example, as non-linear gradients in terminal electron acceptors (TEAs) and substrate concentrations develop over time, ecosystems may experience either rapid losses in C as carbon dioxide (CO_2) and/or methane (CH_4) or experience delays in response to wetting/drying (Joos et al., 2010). As oxygen is depleted upon abrupt wetting or over an extended saturation period, soil respiration is generally predicted to proceed by sequential consumption of nitrate, manganese, iron, and sulfate and ultimately, methanogenesis. How quickly these competitive processes develop from an initial pool of TEAs and substrate concentrations, and if and how they are switched or become limited as moisture regimes shift are underexplored in wetland soils understood. As shifts in TEAs and products of microbial metabolism are integral to determining the temporal dynamics of measured processes, they will, in turn, determine the dominant C loss mechanisms from a soil system. Recent studies ascribe soil C efflux responses to moisture perturbations to "soil moisture legacy effects" (Evans and Wallenstein, 2012; Banerjee et al., 2016) contingent on the extremity and duration of the perturbation. The few studies on the impact of shifting precipitation regimes (extreme wetting and drying) on soil microbiome have focused on upland systems by analyzing microbial community composition (Kieft et al., 1987; Xiang et al., 2008; Evans and Wallenstein, 2012; Barnard et al., 2015) or have concentrated on identifying statistical associations between the microbial and chemical data, e.g. electron acceptor concentrations (Cong et al., 2015). Here, using controlled laboratory incubations, we investigated the degree to which extreme moisture conditions could alter process rates. We developed a conceptual model of competing processes using TEA and metabolite profiles, and the thermodynamic potentials of key processes. Our goal was to use these data types to examine the potential for unquantifiable pathways key to C cycling and/or stress response with rapidly fluctuating moisture, and identify factors that govern the dominant C loss processes in hydrologically influenced soil systems.

We sought to investigate how limitations in TEAs and metabolites central to anaerobic C cycling control the relative dominance of sulfate reduction, iron reduction and methanogenesis in these ecosystems. We hypothesized that (i) an extended saturation will create a "legacy" of conditions primed to increased C loss via methanogenesis (ii) drying of previously saturated soils will induce aerobic C oxidation pathways, and cause osmolytes production, and (iii) wetting of previously dry soil will result in a lag phase in the onset of anaerobic microbial metabolism. Thus, we used controlled laboratory incubations of soils from a tidal wetland in southwestern Washington State (USA) to investigate the degree to which extreme moisture conditions could alter process rates, TEAs, metabolite profiles and thermodynamic potential of competing processes. These data types revealed the potential for unquantifiable pathways key to C cycling and/or stress responses to rapidly fluctuating moisture; from this we developed a conceptual model of the key biogeochemical processes based on observed and estimated stoichiometric relationships between metabolite profiles and TEAs in response to antecedent soil moisture. Such a model construct based on controlled laboratory studies provide process knowledge at a resolution otherwise difficult to obtain from field-based observations.

2. Materials and methods

2.1. Site description and soil collection

One of the largest remaining wetland complexes on the West Coast of the continental United States is on the lower Columbia River and estuary, a 234 km, tidal-fluvial continuum between the Pacific Ocean and Bonneville Dam. The freshwater wetland site is at the widest part of the lowland Columbia near the ocean, at river-kilometer 37 on Grays Bay. The difference between the maximum higher high and minimum lower low for the sampling year (1 Jan–31 Dec 2015) was 3.44 m based on predicted water levels (NOAA, 2017). Grays Bay is in the Energy Minimum reach of the Estuary system zone, near the boundary between tidal freshwater and brackish vegetation zones, where hydrodynamics are strongly affected by both the mixed semi-diurnal tidal regime and river flows (Jay et al., 2016). The Sitka spruce (*Picea sitchensis*) freshwater forested wetland type at the site is characterized by a step-pool channel system where pools alternate with natural log jams and dams built by the North American beaver (*Castor canadensis*) (Diefenderfer and Montgomery, 2009). Modeling indicates that surface water may exceed the bankfull elevation of 2.5 m North American Vertical Datum of 1988 (NAVD 88) as frequently as 17.4% of the time (Coleman et al., 2015). Groundwater dynamics have not been characterized but are assumed to be complex because of the complex channel system and microtopography (Diefenderfer et al., 2008), as well as the root structures of woody plants. At present, the elevation range at which we have surveyed rooted herbaceous, shrub and tree species at the site is 1.8 m to 3.6 m NAVD88 (Borde et al., 2011). The dominant plant species in the 3 m^2 sampling area selected for this study is the obligate wetland plant skunk cabbage (*Lysichiton americanus*), and the sampling area is fringed with salmonberry (*Rubus spectabilis*). The elevation range at which we have surveyed skunk cabbage below river kilometer 70 on the Columbia is 1.9 m to 3.4 m NAVD 88 (Diefenderfer et al., 2013). Of the approximately 8.91 km^2 of the Sitka spruce forested wetland that remains on the Columbia River floodplain (Christy and Putera, 1992), the Secret River forested wetland measures 0.5 km^2 (Coleman et al., 2015). We restricted soil sampling to a relatively small area in order to constrain effects of spatial heterogeneity in micro-elevation driven soil saturation levels for the laboratory investigation.

A grid sampling technique was used to collect soil cores (2.5 cm dia. x 5 cm height) from the mineral horizon after removing the organic layer to a depth of approximately 10 cm. The area of interest (3 m^2, as described above) was divided in to 25 × 25 cm^2 grid cells; 3–4 random samples could be collected from each grid-cell to avoid roots in this densely vegetated area. The cores were carefully lifted out, covered with ethanol-sterilized aluminum foil, stored on ice and transported to the Pacific Northwest National Laboratory, Richland, USA, where they were stored at 4 °C until further use.

Fifteen intact cores were randomly chosen for this study. The average bulk density of the silty soil was 0.97 g cm^{-3}. An experimental unit consisted of a PVC receiving column fitted with two sterilized stainless steel screens (2 and 50 μm openings) placed at the bottom, and closed with PVC caps on both ends (Fig. S1). A sterilized blue-butyl stopper (Bellco Glass Inc.) fitted the top cap was used for headspace gas sampling. All parts in contact with soil were sterilized by autoclaving or by flame sterilization using 80% ethanol.

2.2. Laboratory incubation study

Intact soil cores were subjected to three treatments: two fluctuating moisture regimes to test the effect of antecedent moisture and a continuous saturation/anoxic condition. Cores were pre-incubated at 20 °C for 18 days, and measured daily for headspace CO_2 and CH_4 production rates. At the end of pre-incubation, cores were randomly assigned to the three treatment incubations: Wet-Dry (n = 5), Dry-Wet (n = 4) and continuous Saturation (n = 3). Cores (n = 3) for time-zero (t0) analysis of water-extractable metabolites, sulfate and nitrate concentrations were processed, as described in sections 2.5 and 2.6, within 4 h of end of pre-incubation. Sub-

samples from t0 cores were also analyzed for particle size and concentrations of total Fe, Mn and Mg (Table S1).

After onset of treatment conditions, samples were maintained under controlled atmosphere inside a biological safety cabinet at 25 °C for 120 days. Samples were kept under a microaerophilic (more representative of the *in situ* condition) headspace for the first 14 days to encourage a gradual shift towards the target redox extremes, *i.e.* aerobic vs. anoxic. For the wet phase (39 days) of the Wet-Dry treatment, during which the goal was to stress the soil microbes and force the communities to shift along the redox ladder, samples were allowed to imbibe water (sterile de-ionized and de-gassed water) by capillary action until saturated (~16 h) and an additional volume (1–2 ml) of water was added from the top using a sterile pipette to ensure ~1 mm of standing water on the soil surface; headspace was anoxic (Ar purged) after the first 14 days. During the contrasting dry phase (80 days) of this treatment, samples were gradually dried by evaporation under an aerobic headspace, to a constant weight, and maintained as such until end of incubation. Similarly, during the dry phase (39 days) of the Dry-Wet treatment, field-moist samples were allowed to dry by evaporation under aerobic conditions for an additional 25 days after the initial microaerophilic incubation.

We analyzed the respiration data to identify significant shifts in microbial activity. When respiration rate decreased significantly in the Dry–Wet treatment (after day 39), we reversed conditions to test the effect of the legacy of the antecedent dry condition on a new moisture state (also see section 3.1). This indicated that microbial activity was significantly diminished and the community metabolic state had significantly shifted from t0. Therefore, to test the effect of the "legacy" of the antecedent wet condition on a new moisture regime, we reversed conditions: the Wet-Dry samples were now subjected to air-drying under aerobic conditions; the Dry-Wet samples were wetted by addition of de-gassed sterile de-ionized water until the rate of evaporative loss was lower than the volume of water added and incubated under anoxic headspace (Ar). The incubations were ended after waiting out the lag phase in methanogenesis as observed in the Saturation treatment described below.

Samples for the Saturation treatment were maintained under microaerophilic headspace for 14 days, after which they were maintained under anoxic conditions (Ar purged) until end of incubation. This treatment was monitored for evidence of methanogenesis.

Daily gas measurements for headspace CO_2 and CH_4 in all samples were carried out for 65 days and then every 5 days for up to 120 days. After headspace sampling during the wet/saturation conditions, the experimental units were adjusted for water content and the headspace purged with Ar. Samples during the dry phases were capped for at least 2 h before headspace gas sampling. To maintain and control water content, experimental units were monitored gravimetrically daily for up to 65 days and every 5 days thereafter. At the end of incubation (120 days), the units were destructively sampled. Soil was processed inside a glove bag (Coy Laboratories, O_2 < 5 ppm, 2.1% H_2): soil cores were extruded from the PVC columns sieved (<4 mm), homogenized, and subsampled for chemical analyses. Samples were stored at −20 °C until further processing.

2.3. Gas chromatography

Headspace gas was analyzed with a Agilent 6890 gas chromatograph equipped with a methanizer and Flame Ionization Detector with a Restek Rt®-Q-BOND (30m, 0.32 mm i.d., 10 um d.f.) column. Details of chromatography method are provided in Supplementary Section 2.1. Dissolved gas (CO_2 and CH_4) concentrations were calculated based on headspace measurements after correcting for soil volume, water content and Henry's law solubility constants as previously published (Lide and Frederikse, 1995; RoyChowdhury et al., 2015). Final concentrations are reported as μmol g^{-1} dry weight (dwt.) soil ± standard error.

2.4. Ion chromatography analysis of dissolved terminal electron acceptors

Water soluble anions fluoride (F^-), chloride (Cl^-), Bromide (Br^-), nitrate (NO_3^-), nitrite (NO_2^-) and sulfate (SO_4^{2-}) in soil were measured to estimate treatment effects on dissolved electron acceptor pools and conductivity. Wet soil (~2 g) from microcosms (five technical replicates) were extracted with 10 ml de-ionized water for 12 h at 4 °C on a mechanical shaker. The extracts were centrifuged at 2500 × *g* for 15 mins. at 4 °C and filtered through 0.2 μm polyethersulfone membrane filters (Pall Corporation). Extracts were stored at −20 °C until analyses on an ion chromatograph. Samples were run on a Dionex ICS-2000 anion chromatograph with AS40 auto sampler using an isocratic method as previously described (Zachara et al., 2016). Details of analytical methods and standard ranges are reported in Supplementary Section 2.2. We used the concentrations of SO_4^{2-} thus obtained to calculate potential reduction rates from chromium-reducible-$^{35}SO_4^{2-}$ reduction assay conducted using homogenized soil slurries (1:1, w:v) following previously published methods (Fossing and Jorgensen, 1989, 1990).

2.5. Extracellular metabolite analysis using proton-NMR

Samples for NMR analyses of extracellular/water soluble metabolites were prepared as described in Section 2.4 above. Metabolites were identified and their concentrations quantified using ^1H NMR according to published data collection guidelines (Weljie et al., 2006). Detection limit of the method was 1 μM. Specific details on the previously published protocol (Daly et al., 2016) are reported in Supplementary Section 2.3. Metabolite concentrations are reported as μmol g^{-1} dry weight of soil. Analytes of interest included short-chain fatty acids, alcohols as fermentation products and any signatures of osmolytic stress relevant to drought conditions.

2.6. Mass balance calculations

We calculated mass balances of metabolites involved in six pathways linking oxidation of butyrate, propionate, formate, and ethanol to acetate (Fig. 5a–c) to predict acetoclastic methanogenesis using known stoichiometric reactions (Thauer et al., 1977) and assumed a 1:1 relationship between substrates and products. We also considered the possibility for methanogenesis from formate and H_2. The unknown source of CO_2 was calculated as the discrepancy between calculated flow of CO_2 and measured $\sum CO_2$ at the end-points. The amounts of accumulated metabolites were converted into equivalents of CH_4 according to the stoichiometry of the respective syntrophic pathways (Chin and Conrad, 1995).

2.7. Thermodynamic drive evaluation of acetoclastic methanogenesis, sulfate and iron reduction

Using a previously described framework (Jin and Bethke, 2002, 2003) we estimated respiration rates using thermodynamic rate law to evaluate factors controlling metabolic rates (see Supplementary Section 2.4, Table S3). Acetate was consistently present in high amounts (>150 μmol g^{-1} dwt.) and is the most common organic substrate used by SO_4^{2-} reducers (Winfrey and Ward, 1983), iron (Fe(III)) reducers (Lovley and Klug, 1982), and methanogens (Conrad, 1999) in many environments (Madigan et al., 2000). To

assess possible co-occurrence of these competing processes, we calculated the Gibbs energy of reaction corresponding to these three acetate-dependent processes. The energy available (ΔG_{redox}) to a microbial species in its chemical environment depends largely on the preferred terminal electron acceptor. The available energy (ΔG_{redox}) for methanogenesis in reaction 2 (Table S3) was calculated from the previously reported standard Gibbs free energy (ΔG^{o}_{redox}) (Thauer et al., 1977). ΔG_{redox} for sulfate reduction reaction 3 (Table S3) was calculated using previously published (Ozuolmez et al., 2015) standard Gibbs free energy (ΔGo_{redox}) of reaction estimated from reported thermodynamic parameters (Lever, 2012). The free energy change in synthesizing ATP from ADP and P_i (phosphorylation potential, ΔG_p in equation 1 below) is ~50 kJ mol−1 ATP under typical cellular conditions (White, 1995). Finally, we calculated discrepancies in the net acetate consumption assuming CH_4 and CO_2 as the final sink.

2.8. Statistical analyses

Gas production, anion and metabolites data were analyzed by accounting for the unequal sample size between treatments. Outlier detection for anions and metabolites were performed using Tukey's method to identify samples that ranged above and below the 1.5 times interquartile range. Differences in anion and metabolite concentrations between the treatment groups, viz. Wet-Dry, Dry-Wet and Saturation were tested by Kruskal-Wallis test at the 0.05 level of significance. A post-hoc pairwise comparison was performed using Bonferroni's correction.

3. Results

3.1. Soil respiration

The rate of CO_2 evolution in the Wet-Dry samples increased gradually over time during the wet phase reaching a maximum on day 21 (2.48 μmol g^{-1} d^{-1}) after which a gradual decline in rate was observed with the exception of a large increase at 6.73 μmol g^{-1} d^{-1} on day 33 (Fig. 1a). Overall, CO_2-C loss under wet conditions was significantly higher than under dry conditions. Cumulative CO_2 loss during the wet phase of the Wet-Dry treatment was 7.72 μmol g^{-1} dwt., more than twice the amount lost during the dry phase (3.49 μmol g^{-1} dwt.) (Fig. 1b). The samples under Dry-Wet treatment lost ~8 times more CO_2 (22.2 μmol g^{-1}) under wet conditions (second phase) than under the initial dry phase (2.84 μmol g^{-1}). During the comparable second phase of the continuously saturated samples, we calculated the cumulative CO_2 loss to be ~4 times higher at 67.7 μmol g^{-1} compared to that during phase one (15.2 μmol g^{-1}).

CO_2 concentrations increased immediately upon setting the initially wet samples to dry (day 39) under aerobic conditions and sustained high concentrations for ~72 h (9.42 μmol g^{-1}, $r^2 = 0.91$) before gradually declining to near detection limit concentrations (0.01%) within 45 days (Fig. 1b).

Cores subjected to the Dry-Wet treatment started out under field-moist, microaerophilic conditions and gradually dried to constant weight within 3 days by evaporation under aerobic headspace at 25 °C. Respiration gradually increased reaching a maximum on day 13 (1.15 ± 0.227 μmol g^{-1} d^{-1}) after which there was a rapid decline in CO_2 evolution to 0.548 ± 0.137 within <12 h. After 39 days, soil respiration rate in the dry phase of the Dry–Wet treatment decreased to 54.68 ± 2.07 nmol g^{-1} d^{-1}, nearly 18-fold drop in rate from that on day 14 after exposure to aerobic headspace (1007.27 ± 187 nmol g^{-1} d^{-1}) (Fig. 1a). At this point, we reverse the moisture condition. Upon rapid re-wetting of the dry cores, significant increase in respiration rates was detected. CO_2 concentrations

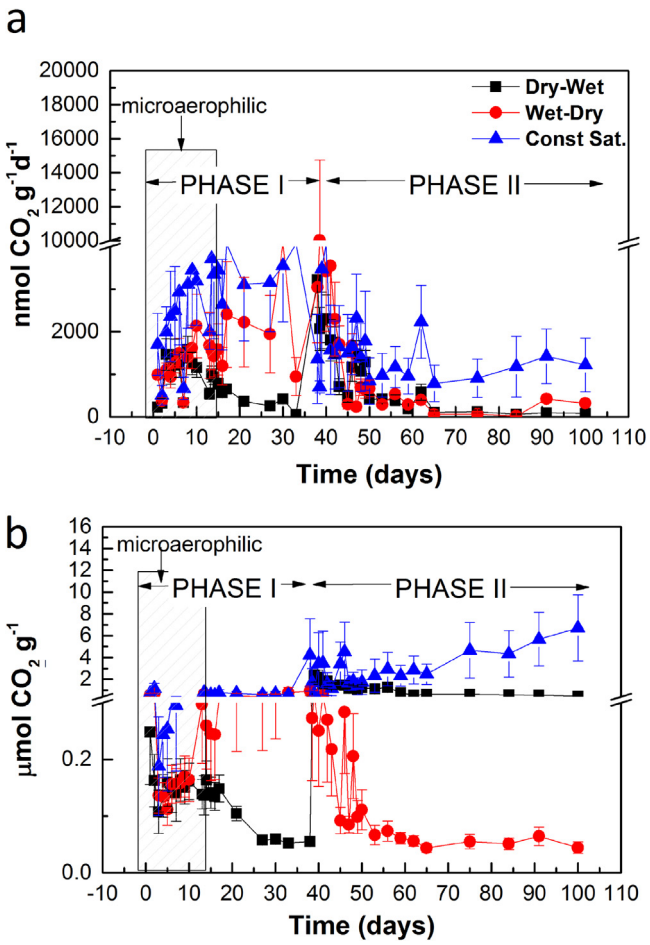

Fig. 1. Temporal dynamics of soil respiration in response to moisture. a. Rates (nmol g^{-1} d^{-1}) and b. Cumulative CO_2 evolution from soils subjected to Dry-Wet (solid black squares), Wet-Dry (solid red circles) and continuous Saturation (solid blue triangles). (For interpretation of the references to colour in this figure legend, the reader is referred to the web version of this article.)

increased from 0.0551 ± 0.00196 to 0.443 ± 0.106 μmol g^{-1} within 12 h and to 2.31 ± 0.566 μmol g^{-1} within 24 h (Fig. 1b). There was a sharp decline in CO_2 at a rate of 0.151 μmol g^{-1} d^{-1} up to day 45 after which a gradual decline continued till the end of incubation, i.e. 120 days. CO_2 produced in cores under continuous saturation (anoxic headspace) increased linearly from day 3 to up to day 13 at a rate of 23.8 μmol g^{-1} d^{-1} and dropped considerably after day 14 maintaining nearly constant concentrations up to day 38. Respiration rates continued to decrease non-linearly after that.

3.2. Methane production

A large variability in CH_4 production was evident between the replicate cores under saturation. One replicate produced CH_4 immediately (Core F6a, Fig. 2) and a second replicate (core B4b, Fig. 2) exhibited a lag phase of approximately 40 days before any CH_4 could be detected in the headspace. No CH_4 gas was detected in the Wet-Dry or Dry-Wet treatments.

The highest rates of CH_4 production detected in core F6a was 2545 nmol g^{-1} d^{-1} after 23 days of incubation while that in core B4b was 228 attained after 7 days of being methanogenic (Fig. 2a). The rate declined gradually over the next 20 days. An increase in CH_4 production rates was observed in both cores after approximately 80 days of incubation. We did not detect CH_4 in the third replicate (core D4a) which limited us from performing any formal statistical

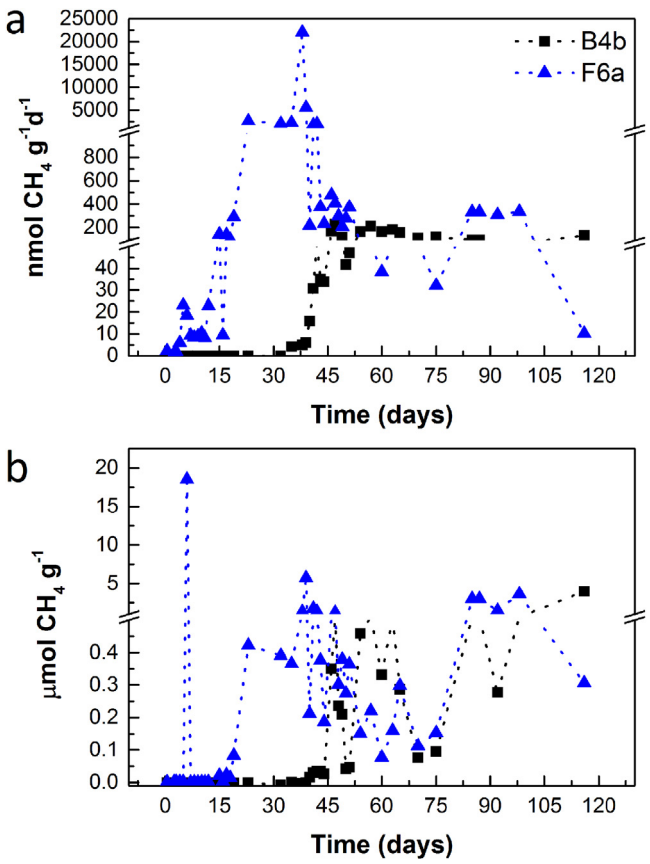

Fig. 2. Temporal response of methane production under saturation conditions. a. Rate (nmol g^{-1} d^{-1}) and b. Cumulative methane production in two biological replicates under constant saturation treatment for 120 days. Individual cores are identified and data not presented as means due to the high variability in methane production lag times and rates.

tests for this treatment. Data from individual cores are presented without averaging to show variability between cores.

3.3. Potential sulfate reduction

We measured potential SO_4^{2-} reduction rates (nmol g^{-1} d^{-1}) in all samples at the end of incubation (data presented in Supplementary Section 3). There was a large variability in the data with only two samples from Saturation treatment (cores B4b (67.6) and D4a (53.8)) and one sample from the Dry-Wet treatment (Core G3a) exhibiting detectable SO_4^{2-} reduction. We were limited by insufficient sample numbers for statistical comparison and use the data only for drawing inferences as discussed below.

3.4. Dissolved terminal electron acceptor concentration

We detected significant effects of treatments on the concentrations of nitrate (NO_3^-), nitrite (NO_2^-) and sulfate (SO_4^{2-}) at the end of incubation (Fig. 3). Concentrations of SO_4^{2-} were significantly higher at the end of the 40 day dry phase than after an equally long wet (p = 1.7e-05) or 120 days of saturated (p = 5.7e-07) conditions. Concentrations of NO_2^- were significantly higher in the wet compared to the dry (p = 0.008) and saturation (p = 0.014) conditions in which case the concentrations were close to the limits of analytical detection. In addition to these dissolved terminal electron acceptors, we measured F^-, Cl^- and Br^- concentrations, the latter of which increased significantly at the end of the dry phase.

3.5. Extracellular metabolite concentrations

A large number of metabolites, including amino acids and fermentation products like short-chain fatty acids significantly increased under wet conditions (Fig. 4 and Table S2). Metabolites detected uniquely at the end of dry phase included low levels of isoleucine, leucine and trehalose (0.1 µmoles) (Fig. 4b). Glycine was also significantly higher at the end of the dry phase (p = 0.0001).

The most abundant fermentation intermediates detected at the end of incubation included butyrate, ethanol, propionate, formate and acetate with concentrations ranging from 15 to 200 µmoles g^{-1} (Fig. 4a). Acetate was the second most abundant metabolite followed by acetone in the Wet-Dry and Saturation treatments, and these two metabolites maintained approximately 1:1 stoichiometry. Acetone was higher in the wet versus the dry (p = 0.0006) or saturation (p = 0.0003) conditions indicative of active fermentation upon re-wetting. Acetate concentrations were higher under wet (p = 0.04) than under dry conditions and no significant difference was observed between the wet and saturation conditions. Isopropanol was consistently found in concentrations an order of magnitude greater than the other metabolites (>1 mmol g^{-1} soil). Due to large inter-core variability in CH_4 production rates reported above, we further examined the variability in the extracellular metabolite concentrations in these cores. Pairwise comparisons showed significantly higher concentrations of acetone, and caproate, formate, isobutyrate and uracil in the two methanogenic cores F6a and B4b. In contrast, core D4a had higher methanol concentrations (Fig. S2).

4. Discussion

We had challenged the paradigm of soil moisture "legacy effect" that antecedent soil moisture conditions determine the dominant C loss pathways in an altered moisture regime. This would mean that energetically favorable oxidative reactions persist upon re-wetting dry soils while anaerobic C loss pathways would drive C loss upon drying previously saturated soils. Because moisture and redox conditions are intricately related, our effort was to deconvolute them by tracking changes in TEA and metabolites central to anaerobic C cycling. We examined these processes by subjecting soils sampled from a coastal wetland to extreme hydrologic perturbations to develop a pathway-level understanding of how hydrologically-driven processes are linked, and to identify the coupled processes most sensitive to future extremes of hydrologic regimes.

4.1. Potential for co-occurrence of acetate-dependent anaerobic pathways

Changes in TEA availabilities and metabolite profiles were better indicators of a system's resilience to change than a summative measurement like community respiration rate dynamics. We observed that the effect of rapid drying or re-wetting on soil respiration rates was short-lived and the relationship of soil C efflux (CO_2 and CH_4), with moisture was non-monotonic. Cumulative C lost during the wet/saturated phases was significantly higher than during the dry phase. Using a combination of empirical observations and theoretical derivations, we showed that the soil system had potential for co-occurrence of acetotrophic SO_4^{2-} reduction, acetate-dependent Fe(III) reduction and acetoclastic methanogenesis.

We could not account for acetate consumption due to methanogenesis alone, as indicated by the unknown sinks (Fig. 5a–c). Thermodynamic calculations showed that oxidation of accumulated alcohols, e.g. ethanol and propanol, to acetate were exergonic. Acetate is the most important precursor for methanogenesis, theoretically accounting for >67% of CH_4 production when polysaccharides are anaerobically degraded (Conrad, 1999). We

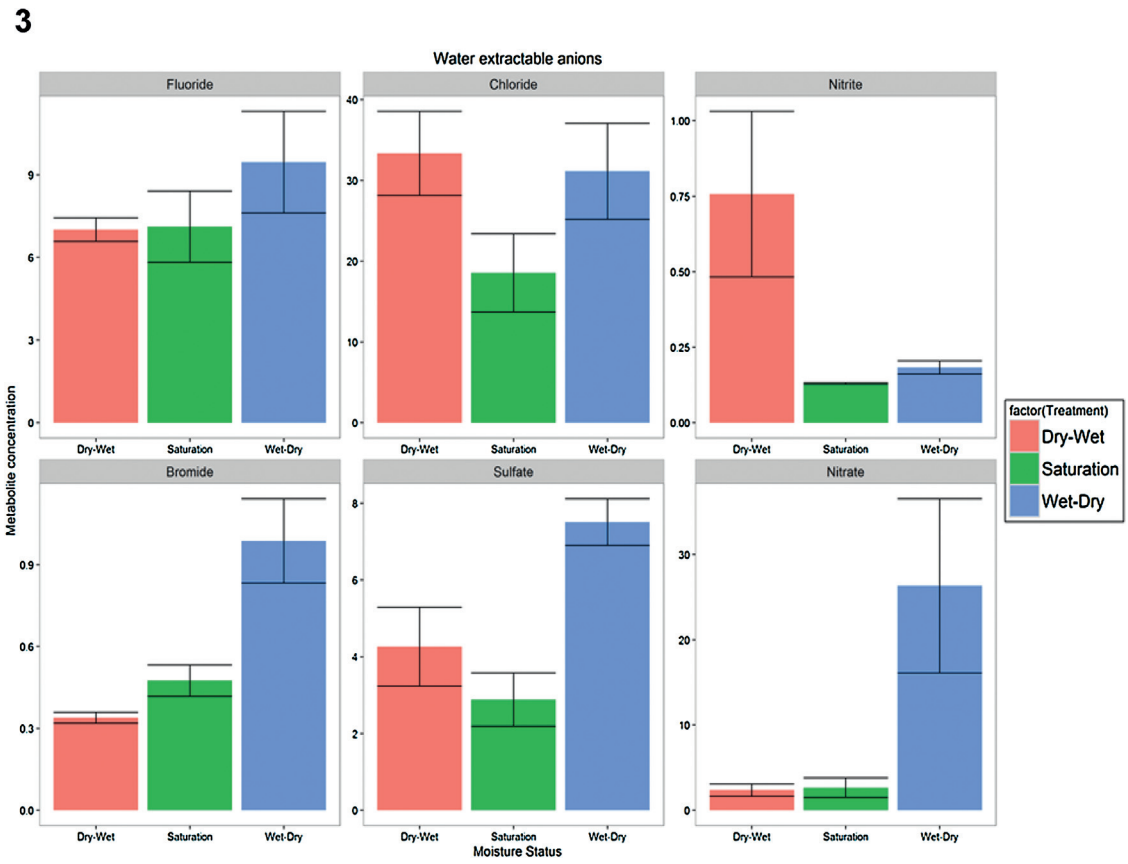

Fig. 3. Effect of moisture condition on concentrations of major dissolved anions in soil extracts.
Concentrations were measured in ppm and are reported μmol g^{-1} soil dry weight. Measurements were obtained from the end-of-incubation samples (t = 120 days). Whiskers indicate the most extreme values within 1.5 multiplied by the interquartile region; values outside that range (outliers) are represented by circles. Box: 25% quartile; median, 75% quartile. Note the differences in scale of the y-axis. Pairwise comparison of means to test treatment effects were performed after outlier removal.

therefore estimated the thermodynamic potential for otherwise difficult-to-quantify pathways, e,g. acetotrophic SO_4^{2-} reduction, acetate-dependent Fe(III) reduction and acetoclastic methanogenesis, to assess competition for acetate as the primary electron donor. Surprisingly, mass balance calculations for measured fermentation products and methanogenesis precursors did not account for the net acetate pools in our treatments. Thus we hypothesize that pathways leading to acetogenesis are important in this ecosystem and might outcompete consumption of acetate constrained by TEA sink strengths.

Based on calculated rates we inferred that acetotrophic SO_4^{2-} reduction could be an active process under wet/saturated conditions. However, our results show that thermodynamic factors may exert significant control on acetotrophic SO_4^{2-} reduction, and must be considered in addition to kinetic estimates to predict rate laws. For example, thermodynamic potential factors (F_T) were significantly lower than unity under saturation ($F_T = 0.01$) and wet ($F_T = 0.006$) conditions, indicating that the available energy (ΔG_{redox}) was close to the conserved energy (ΔG_p) (see Supplementary Section 2.4). This would suggest that little energy is available for the sulfate reducers to carry out the process. In contrast, we obtained a negative value under the dry condition ($F_T = -0.02$) indicating that the available energy is lower than that required to synthesize ATP which, in turn, means cessation of SO_4^{2-} respiration. These theoretical considerations provide indirect evidence for the sensitivity to fluctuating moisture. This is significant as SO_4^{2-} reduction is energetically favored in the competition for methanogenesis substrates and can mitigate methane flux from wetlands (Gauci et al., 2004). Future studies should empirically capture these limiting factors using higher temporal resolution.

Interestingly, calculated rate constants indicated that acetotrophic SO_4^{2-} reduction could be a major process leading to C loss in this soil system. Although SO_4^{2-} concentrations in our samples were low (~10 μM g^{-1} dwt.) compared to other freshwater systems (10–>500 μM) (Lovley and Klug, 1983; Pester et al., 2012), they were within the range of half saturation constants (*Km*) of 5–30 μM for acetotrophic SO_4^{2-} reduction (Ingvorsen et al., 1981; Smith and Klug, 1981; Bak and Pfennig, 1991). We calculated the relative rates of SO_4^{2-} reduction under the three treatments using product of the dual Monod equation (Widdel, 1988) and published F_Ts (Jin and Bethke, 2005). Notably, the calculated relative rates under saturation (76 nmol g^{-1} d^{-1}) and Dry-Wet (61 nmol g^{-1} d^{-1}) treatments were within the ranges detected in low SO_4^{2-} sediments (Widdel, 1988; Pester et al., 2012) (Canfield et al., 1986; Fossing and Jorgensen, 1990) and the measured rates of potential SO_4^{2-} reduction (nmol g^{-1} d^{-1}) in this study (see Supplementary section 3).

We also determined that acetate-dependent Fe(III) reduction was a thermodynamically favorable process in our incubations. We estimated the rate of Fe(III) reduction assuming that 50% of the total Fe(III) (Table S1) was microbially reducible, as frequently observed in non-rhizosphere soils from freshwater wetlands (Weiss et al., 2004). Based on the stoichiometry for Fe(III) reduction using acetate as the sole electron donor (reaction 4, Table S3), we calculated F_T and reaction rates using ΔG^o_{redox} from literature (Roden and Lovley, 1993). We assumed a net ATP generation per 0.5 mol $(acetate)^{-1}$ (Mahadevan et al., 2006) and *Km* of 0.83 μM (Roden and Wetzel, 2003). We calculated $F_T = 1$ indicating that the reaction is not thermodynamically constrained *i.e.,* the forward reaction overwhelms the reverse. Using a value for maximum rate of biotic Fe(III) reduction at 0.05 μmol ml^{-1} from similar environments (Roden

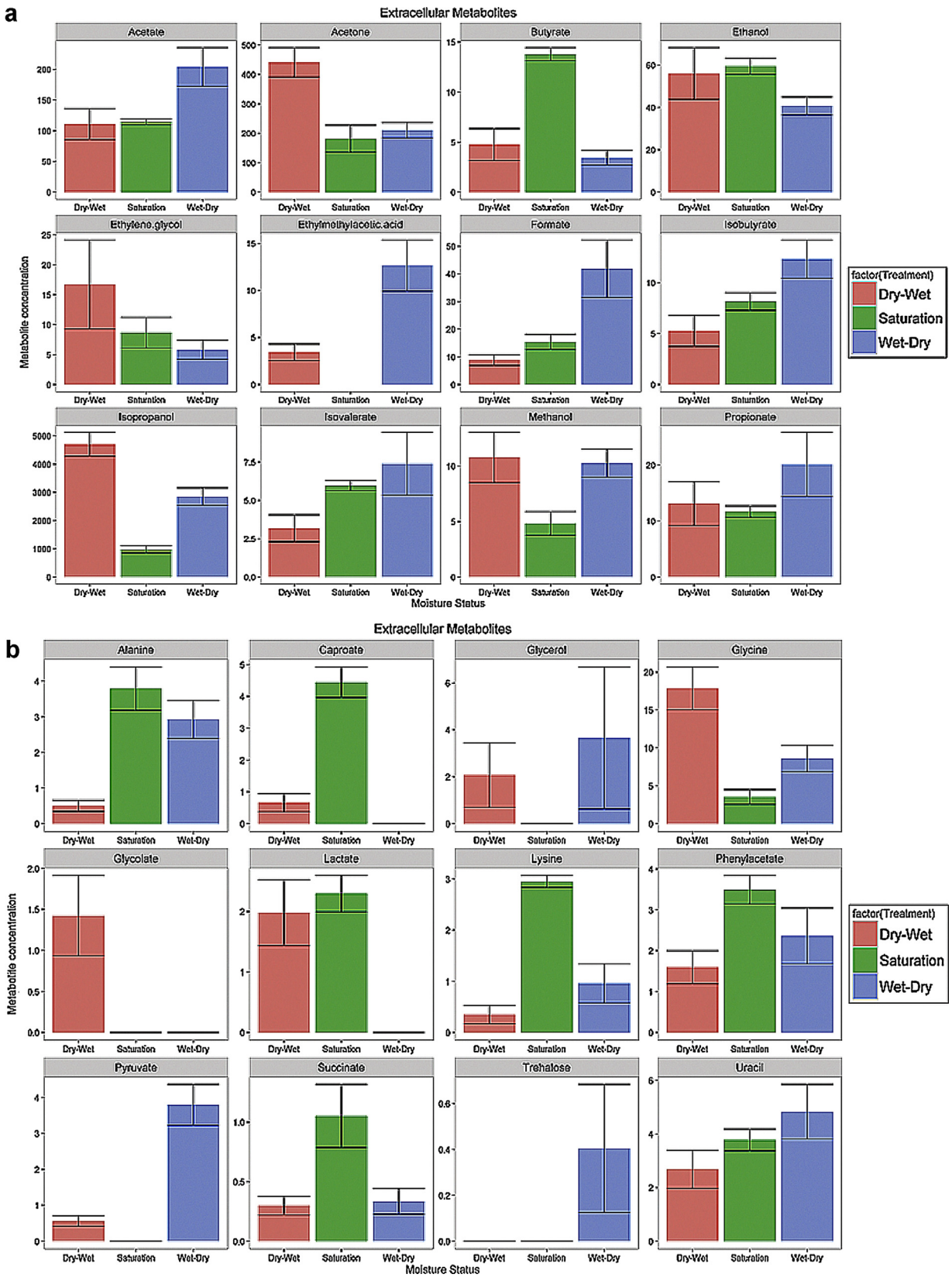

Fig. 4. Effect of moisture conditions on extracellular metabolites.
Concentrations are reported in μmol g^{-1} soil dry weight. Measurements were obtained from the end-of-incubation samples (t = 120 days). Data are presented as bar-plots of means ± standard error in two separate plots to aid visualization of treatment effects on metabolites measured at (a) high and (b) low concentrations. Pairwise comparison of means to test treatment effects were performed after outlier removal. Note the differences in scale.

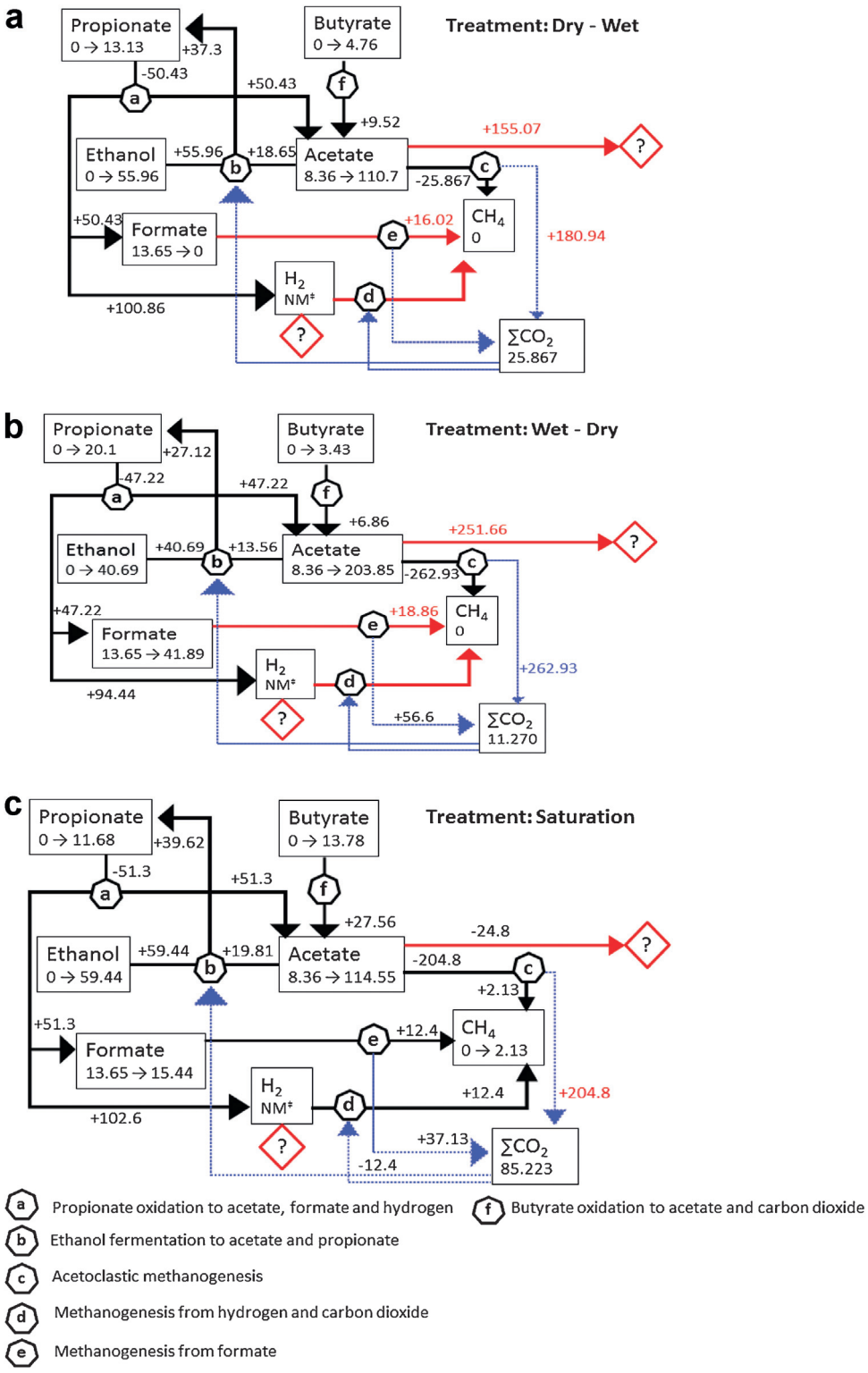

Fig. 5. Mass balance of metabolites central to acetoclastic methanogenesis conducted for three moisture conditions.
a. Dry-Wet, b. Wet–Dry and c. Saturation. Boxes show pool sizes at time-zero → pool sizes at end of incubation; masses are expressed in μmol g^{-1} dwt. Zeros represent analytical limits of detection. Pools of CH_4 and CO_2 are the cumulative concentrations calculated over the 120 day incubation period. Negative and positive numbers respectively indicate masses lost or gained during the incubation. $\sum CO_2$ is the sum of all CO_2 species (gaseous and dissolved). All flows of CO_2 are indicated by blue dotted arrows. Unquantified processes and electron sinks are indicated in red diamonds.
Reactions represented are constrained to the following based on the dominant metabolites:
a. Propionate fermentation to acetate, formate, and hydrogen [$CH_3CH_2COO^- + 2H_2O = CH_3COO^- + HCOO^- + 2H_2 + H^+$;
b. Ethanol fermentation to acetate and propionate [$3(CH_3CH_2OH) + 2HCO_3^- = CH_3COO^- + H^+ + 2(CH_3CH_2COO^-) + 3H_2O$
c. Acetoclastic methanogenesis [$CH_3COO^- + H^+ = CH_4 + CO_2$]
d. Methanogenesis from hydrogen and carbon dioxide [$4H_2 + CO_2 = CH_4 + 2H_2O$]
e. Methanogenesis from formate [$4HCOO^- + H^+ + H_2O = CH_4 + 3HCO_3^-$].
f. Butyrate oxidation to acetate [$CH_3CH_2CH_2COO^- + 2H_2) = 2[CH_3COO^-] + HCO_3^-$
Amount of CH_4 produced from $H_2 + CO_2$ and that from formate have been set as equal because we did not measure the partial pressure of hydrogen in the samples.

and Wetzel, 2002; Whitmire and Hamilton, 2008), we estimated the rate of acetate-dependent Fe(III) reduction to be 0.049 μmol ml^{-1}, less than 20% of that estimated for acetoclastic methanogenesis. The soils studied here are rich in iron and we hypothesize that Fe(III) reduction is a major C loss process setting the principal threshold beyond which the system may become predominantly methanogenic as observed in anoxic soils from diverse ecosystems (Bond and Lovley, 2002; RoyChowdhury et al., 2015). Future studies investigating the competitive interactions between acetate consumers in response to fluctuating moisture should focus on empirical data generation.

Acetoclastic methanogenesis was not substrate-limited under the saturated conditions and both thermodynamically and kinetically favorable. We estimated rates of acetoclastic methanogenesis from the saturated condition using a *Km* of 11.5 μM (Roden and Wetzel, 2003), maximum CH_4 production rate of 0.25 μmol g^{-1} dwt. d^{-1} (Core B4b in this study, Fig. 2) and a calculated F_T close to unity (=0.999). The estimated rate of 0.227 μmol g^{-1} dwt. d^{-1} closely approximated the empirical value suggesting that acetoclastic methanogenesis is a kinetically favorable pathway in this ecosystem. Also, the near-unity value for F_T suggests that the available energy is large compared to the conserved energy and, therefore, the reaction is not thermodynamically limited. Ignoring the thermodynamic potential factor, and using acetate as the electron donor, we estimated comparable CH_4 production rates in Wet-Dry (0.189 μmol g^{-1} dwt. d^{-1}) and Dry-Wet treatments (0.181 μmol g^{-1} dwt. d^{-1}). Since we did not detect any CH_4 in samples under the latter two treatments, we hypothesized that other acetate consumption pathways might be active in these soils. Alternatively, the long lag phase in CH_4 production (>40 days) observed under saturation conditions suggest that the antecedent dry phase prolonged the establishment of complete anoxia and/or depletion of the alternative TEAs upon re-wetting and the system may become methanogenic over extended wet periods. We also note that the long lag phases observed in the Saturation treatment, or no detection of CH_4 in the wet phases of the fluctuating treatments could be an experimental limitation of our static incubations.

The observed accumulation of short-chain fatty acids at the end of dry phases contradicted the expected outcome of accelerated oxidation of these compounds under the energetically favorable aerobic condition. The high levels of formate, acetate, isobutyrate, isovalerate, propionate and pyruvate (10–50 μmoles g^{-1} dwt.) observed at the end of the incubation in the Wet-Dry treatments must have accumulated during the antecedent wet phase. We therefore hypothesize that metabolism of these compounds may have been limited by shifts in microbial community composition or function, by decreased biomass due to death or dormancy upon drying, or by deviations in metabolic pathways preference relating from these compounds.

4.2. Carbon mineralization response to fluctuating moisture conditions

The high rates (μmol g^{-1} d^{-1}) of CO_2 evolution for Wet-Dry (7.92 ± 2.07), Dry-Wet (2.61 ± 0.873) and Saturation (11.5 ± 4.31) treatments within 24 h of the incubation were probably caused by de-gassing of soil pores, as commonly observed due to physical disturbance during sampling and incubation set-up. However, similar ranges in the respiration rates between the wet treatments indicates similar physiological responses of the indigenous microbial community but different rates of recovery to initial conditions.

Cumulative CO_2 at the end of the two drying phases reached similar levels (~3 μmol g^{-1} dwt.) suggesting a threshold for mineralizable C that is accessible to the aerobes in this predominantly saturated environment. At sub-optimal soil moisture, osmotic stress and substrate diffusion are known to limit microbial activity as well as reduce maintenance costs following protein degradation and lower membrane potentials (Schimel et al., 2007; Fuchslueger et al., 2014; Classen et al., 2015) in response to stress. We detected trehalose, a compatible solute known to be a stress indicator (Yancey, 2005), at the end of incubation in the Wet-Dry treatment which supports the microbial stress hypothesis frequently reported in upland soils during the dry phases (Fierer and Schimel, 2003). Upon rewetting, the average respiration rate was 60 times higher than the rate measured 12 h prior to the wetting event and 5 times higher than that measured after 3 days of drying at constant weight. Interestingly, this rate was almost equal to that measured on day 1 of incubation. We did not expect that available organic matter was limited in these soils, although we did not detect measureable amount of glucose or other simple C substrates in the time-zero metabolites. Therefore, the stress mechanism may explain the initial flux of CO_2 upon re-wetting.

The CO_2 production rates during the wet phase of the Wet–Dry treatment were comparable to that under saturation. And, CO_2 efflux increased immediately by 10-fold upon the onset of aerobic drying on day 40. We think this short-term effect is a combined response of accelerated oxidation of labile C released upon microbial stress. Respiration activity decreased over the 120 day incubation. This may be attributed to anoxic microsites formed in these intact cores during the wet phase which would curtail oxidative metabolism (Liesack et al., 2000; Banerjee et al., 2016). Fermentation product accumulation, as described above, supports this hypothesis. Alternately, if the fermentation products persisted from the wet phase, we hypothesize that re-establishment of the "enzymatic latch" prevented activity of phenol-oxidase (Freeman et al., 2001). The enzymatic latch is proposed to lower rates of organic matter biodegradation in anaerobic environments. Both of these possibilities, however, remain to be tested experimentally.

We observed consistently high rates of CO_2 production when soils were saturated and anoxic before starting to decline after ~50 days. It is useful to note here that at least two of the three biological replicates from the Saturation treatment were completely anoxic within 40 days of incubation as evidenced by CH_4 production. The total CO_2 losses during the saturation and wet phases were 20- and 8- times higher than during the dry phases, suggesting that decomposition is very efficient in these anaerobic environments. The cumulative CO_2 loss during the dry phases of the fluctuating treatments were similar indicating that respiration was not limited by nutrients, as seen in increased concentrations of amino acids like glycine, alanine, lysine and methylamines. It is also critical to note that the targeted approach used here to quantify extracellular metabolites production does not reveal all compounds and is likely limited by extraction efficiency and limitations of data analysis. In addition to testing for the temporal dynamics of metabolite profiles in response to moisture fluctuations, future studies should consider using a global community metabolomics approach to obtain further insights in to microbially-driven C cycling in soil systems.

We also identified several CO_2 consuming pathways that could be active in our study, e.g. homoacetogenesis, nitrification, iron and sulfur oxidation. Oxidative acetate dissimilation may be also achieved by using aromatic macromolecules, previously defined as humic acids as primary electron acceptors (Keller et al., 2009). Future studies should, therefore, investigate the C species' sink capacity to serve as ultimate oxidants for acetate using untargeted analytical approaches.

5. Conclusion

We chose a tidally influenced coastal wetland system as our study site based on the premise that the microbially-driven bio-

geochemical processes will be primed to the rapidly fluctuating water levels at the site, and by extension primed to select the energetically favorable metabolic pathways related to carbon cycling. Our objective was not to extrapolate the results to the field or ecosystem scale, but to generate a pathway level understanding of the key processes driving C loss mechanisms to inform future predictive models. To that end, our results illustrate the potential of these tidal wetland sediments to serve as substrates for microorganisms that are capable of catalyzing a range of biogeochemical reactions. Within the reported range of electron acceptor and donor concentrations, the relative importance of homoacetogenesis, methanogenesis, iron reduction, sulfate reduction and methane oxidation in tidal freshwater wetland soils is determined by the rates of organic matter decomposition which, in turn, control the soil C efflux. We show that alternative electron acceptors like nitrate, sulfate and ferric iron may divert C fluxes away from CH_4 production since reduction of sulfate and ferric iron are thermodynamically more favorable than acetoclastic methanogenesis. While we cannot predict the sequence or co-occurrence of the redox processes, we provide evidence for the geochemical and metabolic potential in response to shifting hydrology. The non-linear relationship between soil C efflux and soil moisture suggested that redox rather than antecedent moisture condition determined the directionality and magnitude of change in C loss processes. We, therefore, propose that redox-driven gradients in TEA and metabolite concentrations primarily select for favorable microbial processes, and ultimately govern the amount of C and primary mechanisms of loss.

The sequential reduction of electron acceptors is generally attributed to the different microbes that compete for common electron donors with greater efficiency. It was beyond the scope of this study to measure the competitive interactions between the sulfate reducers, iron reducers, and other processes. Particularly, the conditions under which methanogenesis is activated remains uncertain. It could be that the incubation period was not sufficiently long to deplete all the alternative electron acceptors in this soil, especially that of Fe(III). Future studies will mechanistically investigate the metabolic and trophic interactions that modulate CH_4 production in these ecosystems accounting for the long lag phase in anaerobic processes in response to fluctuating moisture conditions.

Acknowledgements

This research is part of the Microbiomes in Transition Initiative at Pacific Northwest National Laboratory (PNNL). It was conducted under the Laboratory Directed Research and Development Program at PNNL, a multi-program national laboratory operated by Battelle for the U.S. Department of Energy under Contract DE-AC05-76RL01830. A portion of this research was performed using EMSL, a DOE Office of Science user facility sponsored by the Department of Energy's Office of Biological and Environmental Research and located at PNNL.

We are grateful to J. Stegen and A. B. Borde for their assistance in planning the soil sampling trip and in obtaining the soil cores. We are very thankful to S. Fansler for sequencing the samples and to J. Brown for quality checking and processing the raw sequence data. We gratefully acknowledge assistance from K. Weitz with installation of a methanizer on to the gas chromatograph. We thank Blanca Vera Gargallo for her assistance with gas chromatographic analyses of samples. We are thankful to A. E. Plymale for analyzing soil samples for sulfate reduction rate using the radiotracer method and C. Resch for ion chromatographic and ICP-OES analysis of samples.

Publication of this manuscript was assisted by U.S. National Science Foundation grant number 1619948 with project title: U.S. Science International Collaborations and Contributions to EcoSummit 2016 "Sustainability: Engineering Change"

Appendix A. Supplementary data

Supplementary data associated with this article can be found, in the online version, at http://dx.doi.org/10.1016/j.ecoleng.2017.06.041.

References

Bak, F., Pfennig, N., 1991. Microbial sulfate reduction in littoral sediment of lake constance. FEMS Microbiol. Ecol. 85, 31–42.
Banerjee, S., Helgason, B., Wang, L.F., Winsley, T., Ferrari, B.C., Siciliano, S.D., 2016. Legacy effects of soil moisture on microbial community structure and N_2O emissions. Soil Biol. Biochem. 95, 40–50.
Barnard, R.L., Osborne, C.A., Firestone, M.K., 2015. Changing precipitation pattern alters soil microbial community response to wet-up under a Mediterranean-type climate. ISME J. 9, 946–957.
Bond, D.R., Lovley, D.R., 2002. Reduction of Fe(III) oxide by methanogens in the presence and absence of extracellular quinones. Environ. Microbiol. 4, 115–124.
Borde, A.B., Zimmerman, S.A., Kauffman, R., Diefenderfer, H.L., Sather, N.K., Thom, R.M., 2011. Lower Columbia River and Estuary Reference Site Study: 2010 Final Report and Site Summaries, Richland, WA.
Canfield, D.E., Raiswell, R., Westrich, J.T., Reaves, C.M., Berner, R.A., 1986. The use of chromium reduction in the analysis of reduced inorganic sulfur in sediments and shales. Chem. Geol. 54, 149–155.
Chin, K.J., Conrad, R., 1995. Intermediary metabolism in methanogenic paddy soil and the influence of temperature. FEMS Microbiol. Ecol. 18, 85–102.
Christy, J.A., Putera, J.A., 1992. Lower Columbia River Natural Area Inventory, Report to The Nature Conservancy. Washington Field Office, Seattle, WA.
Classen, A.T., Sundqvist, M.K., Henning, J.A., Newman, G.S., Moore, J.A.M., Cregger, M.A., Moorhead, L.C., Patterson, C.M., 2015. Direct and indirect effects of climate change on soil microbial and soil microbial-plant interactions: what lies ahead? Ecosphere 6.
Coleman, A.M., Diefenderfer, H.L., Ward, D.L., Borde, A.B., 2015. A spatially based area-time inundation index model developed to assess habitat opportunity in tidal-fluvial wetlands and restoration sites. Ecol. Eng. 82, 624–642.
Cong, J., Yang, Y.F., Liu, X.D., Lu, H., Liu, X., Zhou, J.Z., Li, D.Q., Yin, H.Q., Ding, J.J., Zhang, Y.G., 2015. Analyses of soil microbial community compositions and functional genes reveal potential consequences of natural forest succession. Sci. Rep. 5.
Conrad, R., 1999. Contribution of hydrogen to methane production and control of hydrogen concentrations in methanogenic soils and sediments. FEMS Microbiol. Ecol. 28, 193–202.
Daly, R.A., Borton, M.A., Wilkins, M.J., Hoyt, D.W., Kountz, D.J., Wolfe, R.A., Welch, S.A., Marcus, D.N., Trexler, R.V., MacRae, J.D., Krzycki, J.A., Cole, D.R., Mouser, P.J., Wrighton, K.C.N.M., 2016. Microbial metabolisms in a 2.5-km-deep ecosystem created by hydraulic fracturing in shales. Nat. Microbiol. 1, 16146.
Diefenderfer, H.L., Montgomery, D.R., 2009. Pool spacing, channel morphology, and the restoration of tidal forested wetlands of the Columbia River, USA. Restor. Ecol. 17, 158–168.
Diefenderfer, H.L., Coleman, A.M., Borde, A.B., Sinks, I.A., 2008. Hydraulic geometry and microtopography of tidal freshwater forested wetlands and implications for restoration, Columbia River, U.S.A. Ecohydrology and Hydrobiology, Ecohydrological processes and sustainable floodplain management opportunities and concepts for water hazard mitigation and ecological and socioeconomic sustainability in the face of global changes, Lodz, Poland, pp. 339–361.
Diefenderfer, H.L., Borde, A.B., Cullinan, V.I., 2013. A Synthesis of Environmental and Plant Community Data for Tidal Wetland Restoration Planning in the Lower Columbia River and Estuary. Pacific Nothwest National Laboratory, Marine Sciences Laboratory, Sequim, WA, for the U.S. Army Corps of Engineers, Portland District, Portland Oregon.
EPA, 2017. US Greenhouse Gas Inventory Report. EPA.
Evans, S.E., Wallenstein, M.D., 2012. Soil microbial community response to drying and rewetting stress: does historical precipitation regime matter? Biogeochemistry 109, 101–116.
Fierer, N., Schimel, J.P., 2003. A proposed mechanism for the pulse in carbon dioxide production commonly observed following the rapid rewetting of a dry soil. Soil Sci. Soc. Am. J. 67, 798–805.
Fossing, H., Jorgensen, B.B., 1989. Measurement of bacterial sulfate reduction in sediments – evaluation of a single-step chromium reduction method. Biogeochemistry 8, 205–222.
Fossing, H., Jorgensen, B.B., 1990. Oxidation and reduction of radiolabeled inorganic sulfur-compounds in an estuarine sediment, Kysing Fjord, Denmark. Geochim. Cosmochim. Acta 54, 2731–2742.
Freeman, C., Ostle, N., Kang, H., 2001. An enzymic 'latch' on a global carbon store – A shortage of oxygen locks up carbon in peatlands by restraining a single enzyme. Nature 409, 149–149.
Fuchslueger, L., Bahn, M., Fritz, K., Hasibeder, R., Richter, A., 2014. Experimental drought reduces the transfer of recently fixed plant carbon to soil microbes

and alters the bacterial community composition in a mountain meadow. New Phytol. 201, 916–927.
Gauci, V., Matthews, E., Dise, N., Walter, B., Koch, D., Granberg, G., Vile, M., 2004. Sulfur pollution suppression of the wetland methane source in the 20th and 21st centuries. Proc. Natl. Acad. Sci. U. S. A. 101, 12583–12587.
IPCC, 2013. The Physical Science Basis: Working Group I Contribution to the Fifth Assessment Report of the Intergovernmental Panel on Climate Change. Cambridge University Press, New York.
Ingvorsen, K., Zeikus, J.G., Brock, T.D., 1981. Dynamics of bacterial sulfate reduction in a eutrophic lake. Appl. Environ. Microbiol., 1029–1036.
Jay, D.A., Borde, A.B., Diefenderfer, H.L., 2016. Tidal-fluvial and estuarine processes in the lower Columbia River: II. Water level models floodplain wetland inundation, and system zones. Estuaries Coasts 39, 1299–1324.
Jentsch, A., Kreyling, J., Beierkuhnlein, C., 2007. A new generation of climate-change experiments: events, not trends. Front. Ecol. Environ. 5, 365–374.
Jin, Q.S., Bethke, C.M., 2002. Kinetics of electron transfer through the respiratory chain. Biophys. J. 83, 1797–1808.
Jin, Q.S., Bethke, C.M., 2003. A new rate law describing microbial respiration. Appl. Environ. Microbiol. 69, 2340–2348.
Jin, Q.S., Bethke, C.M., 2005. Predicting the rate of microbial respiration in geochemical environments. Geochim. Cosmochim. Acta 69, 1133–1143.
Joos, O., Hagedorn, F., Heim, A., Gilgen, A.K., Schmidt, M.W.I., Siegwolf, R.T.W., Buchmann, N., 2010. Summer drought reduces total and litter-derived soil CO2 effluxes in temperate grassland – clues from a C-13 litter addition experiment. Biogeosciences 7, 1031–1041.
Keller, J.K., Weisenhorn, P.B., Megonigal, J.P., 2009. Humic acids as electron acceptors in wetland decomposition. Soil Biol. Biochem. 41, 1518–1522.
Kieft, T.L., Soroker, E., Firestone, M.K., 1987. Microbial biomass response to a rapid increase in water potential when dry soil is wetted. Soil Biol. Biochem. 19, 119–126.
Kirwan, M.L., Megonigal, J.P., 2013. Tidal wetland stability in the face of human impacts and sea-level rise. Nature 504, 53–60.
Kirwan, M.L., Langley, J.A., Guntenspergen, G.R., Megonigal, J.P., 2013. The impact of sea-level rise on organic matter decay rates in Chesapeake Bay brackish tidal marshes. Biogeosciences 10, 1869–1876.
Lever, M.A., 2012. Acetogenesis in the energy-starved deep biosphere – a paradox? Front. Microbiol., 3.
Lide, D.R., Frederikse, H.P.R., 1995. CRC Handbook of Chemistry and Physics, 76th ed. CRC, Boca Raton, FL.
Liesack, W., Schnell, S., Revsbech, N.P., 2000. Microbiology of flooded rice paddies. FEMS Microbiol. Rev. 24, 625–645.
Lovley, D.R., Klug, M.J., 1982. Intermediary metabolism of organic-Matter in the sediments of a utrophic lake. Appl. Environ. Microbiol. 43, 552–560.
Lovley, D.R., Klug, M.J., 1983. Sulfate reducers can outcompete methanogens at freshwater sulfate concentrations. Appl. Environ. Microbiol. 45, 187–192.
Madigan, M.T., Martinko, J.M., Parker, J., 2000. Metabolic Diversity. Prentice Hall, New Jersey.
Mahadevan, R., Bond, D.R., Butler, J.E., Esteve-Nunez, A., Coppi, M.V., Palsson, B.O., Schilling, C.H., Lovley, D.R., 2006. Characterization of metabolism in the Fe(III)-reducing organism Geobacter sulfurreducens by constraint-based modeling. Appl. Environ. Microbiol. 72, 1558–1568.
Martiny, J.B.H., Martiny, A.C., Weihe, C., Lu, Y., Berlemont, R., Brodie, E.L., Goulden, M.L., Treseder, K.K., Allison, S.D., 2017. Microbial legacies alter decomposition in response to simulated global change. ISME J. 11, 490–499.
Ozuolmez, D., Na, H., Lever, M.A., Kjeldsen, K.U., Jorgensen, B.B., Plugge, C.M., 2015. Methanogenic archaea and sulfate reducing bacteria co-cultured on acetate: teamwork or coexistence? Front. Microbiol., 6.
Pester, M., Knorr, K.H., Friedrich, M.W., Wagner, M., Loy, A., 2012. Sulfate-reducing microorganisms in wetlands – fameless actors in carbon cycling and climate change. Front. Microbiol. 3.
Roden, E.E., Lovley, D.R., 1993. Dissimilatory Fe(III) reduction by the marine microorganism desulfuromonas-Acetoxidans. Appl. Environ. Microbiol. 59, 734–742.
Roden, E.E., Wetzel, R.G., 2002. Kinetics of microbial Fe(III) oxide reduction in freshwater wetland sediments. Limnol. Oceanogr. 47, 198–211.
Roden, E.E., Wetzel, R.G., 2003. Competition between Fe(III)-reducing and methanogenic bacteria for acetate in iron-rich freshwater sediments. Microb. Ecol. 45, 252–258.
RoyChowdhury, T., Herndon, E.M., Phelps, T.J., Elias, D.A., Gu, B.H., Liang, L.Y., Wullschleger, S.D., Graham, D.E., 2015. Stoichiometry and temperature sensitivity of methanogenesis and CO2 production from saturated polygonal tundra in Barrow, Alaska. Glob. Change Biol. 21, 722–737.
Schimel, J., Balser, T.C., Wallenstein, M., 2007. Microbial stress-response physiology and its implications for ecosystem function. Ecology 88, 1386–1394.
Smith, R.L., Klug, M.J., 1981. Reduction of sulfur-compounds in the sediments of a eutrophic lake basin. Appl. Environ. Microbiol. 41, 1230–1237.
Thauer, R.K., Jungermann, K., Decker, K., 1977. Energy conservation in chemotrophic anaerobic bacteria. Bacteriol. Rev. 41 (1), 100–180.
Weiss, J.V., Emerson, D., Megonigal, J.P., 2004. Geochemical control of microbial Fe(III) reduction potential in wetlands: comparison of the rhizosphere to non-rhizosphere soil. FEMS Microbiol. Ecol. 48, 89–100.
Weljie, A.M., Newton, J., Mercier, P., Carlson, E., Slupsky, C.M., 2006. Targeted profiling: quantitative analysis of ^{1}H NMR metabolomics data. Anal. Chem. 78, 4430–4442.
White, D., 1995. The Physiology and Biochemistry of Prokaryotes. Oxford University Press.
Whitmire, S.L., Hamilton, S.K., 2008. Rates of anaerobic microbial metabolism in wetlands of divergent hydrology on a glacial landscape. Wetlands 28, 703–714.
Widdel, F., 1988. Biology of Anaerobic Microorganisms. John Wiley & Sons, Inc., New York, NY, USA.
Wieder, W.R., Bonan, G.B., Allison, S.D., 2013. Global soil carbon projections are improved by modelling microbial processes. Nat. Clim. Change 3, 909–912.
Winfrey, M.R., Ward, D.M., 1983. Substrates for sulfate reduction and methane production in intertidal sediments. Appl. Environ. Microbiol. 45, 193–199.
Xiang, S.R., Doyle, A., Holden, P.A., Schimel, J.P., 2008. Drying and rewetting effects on C and N mineralization and microbial activity in surface and subsurface California grassland soils. Soil Biol. Biochem. 40, 2281–2289.
Yancey, P.H., 2005. Organic osmolytes as compatible, metabolic and counteracting cytoprotectants in high osmolarity and other stresses. J. Exp. Biol. 208, 2819–2830.
Zachara, J.M., Moran, J.J., Resch, C.T., Lindemann, S.R., Felmy, A.R., Bowden, M.E., Cory, A.B., Fredrickson, J.K., 2016. Geo- and biogeochemical processes in a heliothermal hypersaline lake. Geochim. Cosmochim. Acta 181, 144–163.